Influence of High-Temperature Aluminizing on the Fatigue and Corrosion Resistance of Nickel Alloy Inconel 740

Ryszard SITEK[1], Dominik KUKLA[2],Akira KOBAYASHI[3] andKrzysztof J. KURZYDLOWSKI[1]

[1)]Faculty of Materials Science and Engineering, Warsaw University of Technology
Woloska 141, 02-507 Warsaw, Poland

[2)]Institute of Fundamental Technological Research, Department for Strength of Materials
Adolfa Pawinskiego 5B Str., 02-106 Warsaw, Poland

[3)]MJIIT, University of Technology Malaysia KL, Jalan Semarak, 54100 Malaysia
& Graduate School of Engineering, Osaka University, Osaka 565 0871, JAPAN

Abstract

The paper presents the results of studies on the structure and properties of the AlNi type diffusion layers fabricated on the IN 740 nickel alloy by chemical vapor deposition using aluminium chloride ($AlCl_3$) introduced into a hydrogen atmosphere. The layers were examined by light microscopy and scanning electron microscopy. Their chemical composition was examined by EDS, and the phase composition - using a Bruker D8 X-ray diffractometer with CuKα radiation. Fatigue tests were carried out in Inconel 740 sample, in the initial state and covered with the diffusion intermetallic AlNi layers. The strength under dynamic load was examined using a MTS 858 testing machine using symmetric load cycles repeated at a frequency of 20 Hz. The stress amplitude was 550 MPa. Corrosion resistance tests were performed employing potentiodynamic methods, in 0.1M Na_2SO_4 solution, at ambient temperature. It is shown that the layers improve the fatigue resistance and corrosion resistance of the Inconel 740 substrate.

Keywords: Inconel 740, CVD, Aluminide layer, High-cycle fatigue, Corrosion resistance

1. Introduction

Inconel alloy 740 has very good mechanical properties (tensile strength at a temperature of about 750°C – below 100MPa) and high corrosion resistance (below 2 mm during 200000h), parameters which are not available with other nickel alloys such as: Inconel 617, Inconel 690, Inconel 718, etc.[1-6)] These properties make it a good choice for the manufacturing of tubing and piping intended for advanced Ultra-Supercritical pulverized coal-fired steam boilers, heated to a temperature of 700°C under a pressure of 375 bar. The use of this material may increase the heat efficiency of the boiler by over 50%[7)]. This alloy has also been investigated in terms of its application for the manufacture of the exhaust valves in automotive diesel engines[8)] and the hottest regions of gas-turbines.

The authors of ref.[9)] suggested that during age-hardening at temperatures between 593°C and 849 °C, Ni_3Ti eta phase platelets form, which may adversely affect the stability of the microstructure and decrease the creep resistance of the alloy. This drawback can be obviated by subjecting the alloys to surface treatments. It has been found that the diffusion-type aluminide layers produced on the alloy surface improve its fatigue strength. This paper presents the results of a study aimed at producing diffusive protective surface layers on an Inconel 740 superalloy substrate using the Chemical Vapor Deposition method.

2. Research Methodology

Layers to be tested were produced on specimens made of the superalloy nickel Inconel 740. The alloy microstructure is shown in **Figure 1** and its chemical composition is given in **Table 1**.

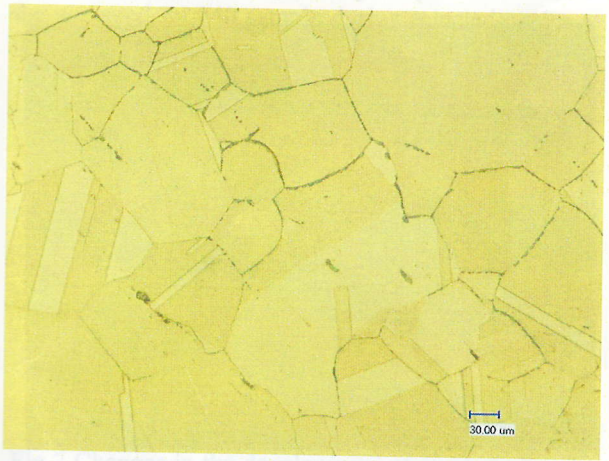

Fig.1 Microstructure of the IN 740 nickel alloy in the initial state.

Table 1 Chemical composition of the Inconel 740 nickel alloy.

Cr	Mo	Co	Al	Ti	Nb	Mn	Fe	Si	C	Ni
25.0	0.5	20.0	0.9	1.8	2.0	0.30	0.7	0.5	0.03	Bal.

The aluminide layers were produced by a chemical vapour deposition (CVD) process using $AlCl_3$ in the atmosphere of hydrogen. The process was conducted at 1020°C under 150hPa for 6 h.

The microstructures of the layers were observed using a scanning electron microscope (SEM), HITACHI SU 70 equipped with a ThernoNoranEDS (Energy Dispersive Spectroscopy) unit. The analysis of the phase composition was performed with an X-ray diffractometer Bruker D8 using CuKα radiation.

The fatigue tests were carried out in a testing machine MTS 858, Model No 359, S/N 1075319, with the axial force range +/- 25 kN, +/- 200 Nm torque moment, equipped with a digital controller TestStar II. The machine was controlled using software MTS TestStar v. 4.0D + TestWare SX-v. 4.0D and a 790.20 Fatigue Test Application. The specimens were mounted using special holders to ensure the alignment of the load and prevent buckling under compression strains. The load was implemented in a mode of force control maintaining zero value of the average force in a cycle and a constant value of the stress amplitude for a given specimen. During the whole process of loading, the change in diameter was measured on the narrowest cross-section of the specimen using an extensometer MTS.

The axial deformation was calculated on the basis of readings of the radial deformations for the assumed value of the Poisson ratio. In all the tests, the frequency was 20 Hz, so that 1 million cycles were implemented during 14 hours. The load was imposed with force control so as to maintain the average force in a cycle at the zero and a constant value of the stress amplitude in a given specimen. A pendulum symmetric load cycle ($\sigma m = 0$) at a frequency of 20 [Hz] was adopted. The fatigue tests were performed within the stress amplitude of 550 (MPa) in the specimens made of the nickel alloy Inconel 740 in the initial state and after the CVD processes.

Corrosion resistance tests were performed employing the potentiodynamic method, using an AutoLab PGSTAT 100 potentiostat in 0.1M Na_2SO_4 solution, at ambient temperature.

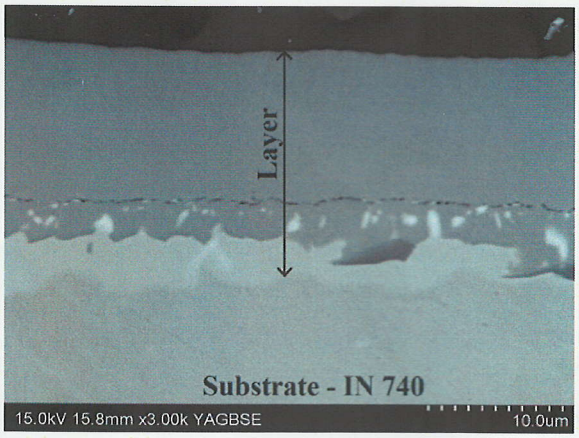

Fig.2 Layer microstructure after low-active aluminizing at a temperature of 1020°C for 6h.

3. Results and Discussion

As a result of the low-active aluminising of the nickel-based Inconel 740 superalloy by chemical vapour deposition, a 30-μm thick diffusive layer was obtained on the entire surface of the specimens (**Fig.2**).

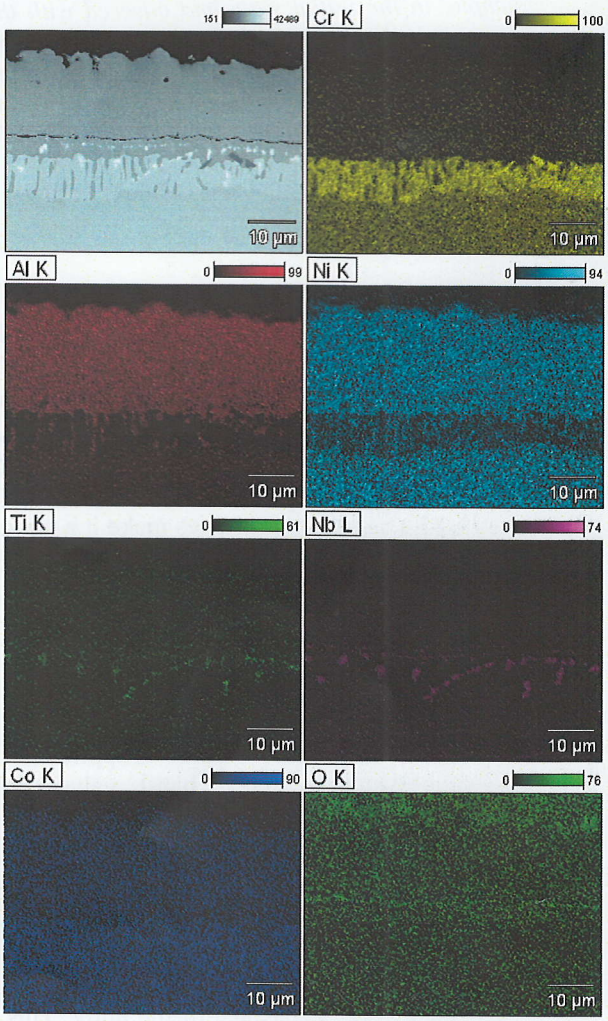

Fig.3 EDS analysis of the chemical composition of a cross-section surface after low-active aluminum deposition at a temperature of 1020°C for 6h.

The mapping of the Ni, Al, Ti, Cr and Nb distributions shown in **Fig.3** indicates that the structure of the layer is complex. X-ray phase analyses (**Fig.4**) show that, after the low-active aluminizing, the layer is predominantly built of AlNi.

Figure 5 shows the results of the fatigue tests in the form of the Wöhler curves obtained for the nickel alloy Inconel 740 in the starting state and after the low-active aluminising processes. One can see changes in the number of cycles up to the specimen rupture against the cyclic tension amplitude. The graphs show well-marked changes in the fatigue parameters in the specimens made of the nickel alloy Inconel 740 subjected to the surface treatment. In the entire range of amplitudes, the number of cycles up to the specimen rapture is lower in the specimens without the aluminide layer.

Figures 6-9 show the results of fatigue tests of the Inconel 740 samples in the starting state (Fig.6 and 7) and after low-active aluminizing (Fig.8 and 9). In Figs.6 and 8 the results are presented in the form of diagrams the fatigue hysteresis development during some selected cycles of fatigue (Fig.6 and 8), and in Figs.7 and 9 - as the variation of strain induced during the successive loading cycles with the differentiation between the average strain value and strain amplitude. **Fig.10** shows the sum of these strains, denoted as the parameter ϕ, as a function of the number of cycles. In the case of both samples we can see the damage development associated with the increase of the average value of strain and it amplitude (Fig.6 and 8). It means, that damage the development is generated by two mechanisms: ratcheting and cyclic plasticity. The development of strain during the successive cycles (Fig.7) shows that, the strain cumulates in an almost linear way i.e. it increases in proportion to the number of cycles.

In the aluminized IN 740 alloy, the stresses due to the damage governed by the, ratcheting and cyclic plasticity mechanisms, were observed within the entire stress amplitude range. The damage underwent changes visible only at medium strains as shifts of the hysteresis loop chiefly towards positive strains. It was only in the final stage of the cyclic loading, when the hysteresis loop is widened, which can be attributed to the activation of the other fatigue damage mechanism i.e. cyclic deformation (Fig.8). The magnitude of the inelastic deformation that occurs during the final loading cycles slightly exceeds that occurring at higher stress amplitudes

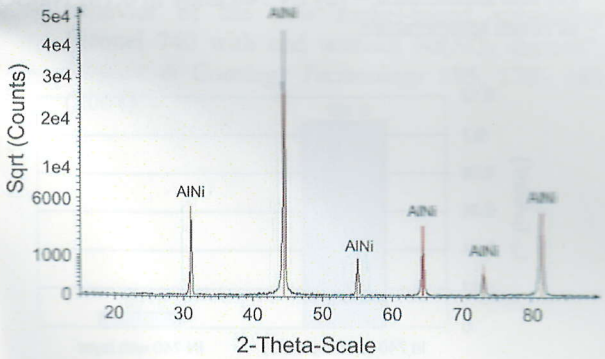

Fig.4 X-ray diffraction pattern of the layer formed on the IN 740 nickel alloy substrate by CVD at 1020°C for 6h.

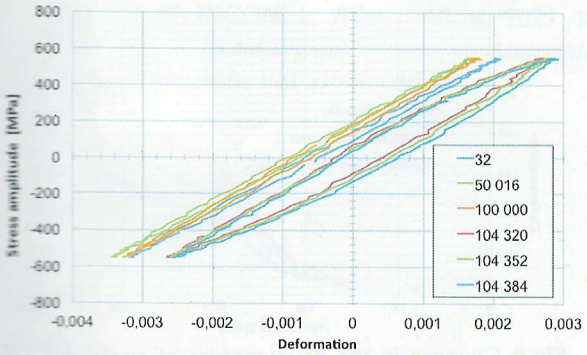

Fig.6 Development of the fatigue hysteresis loop in the uncoated IN 740 sample during selected cycles at the stress amplitude of 550MPa.

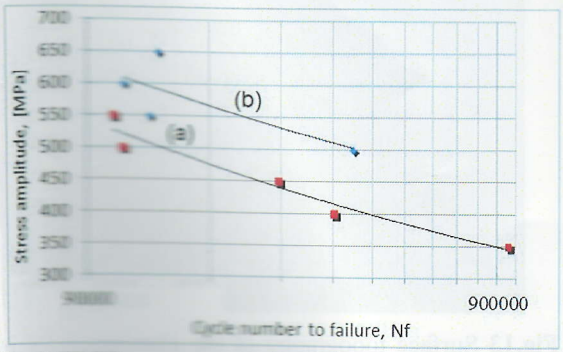

Fig.5 Wöhler curves obtained for the IN 740 nickel alloy: (a) in the initial state, (b) with a AlNi layer produced by CVD.

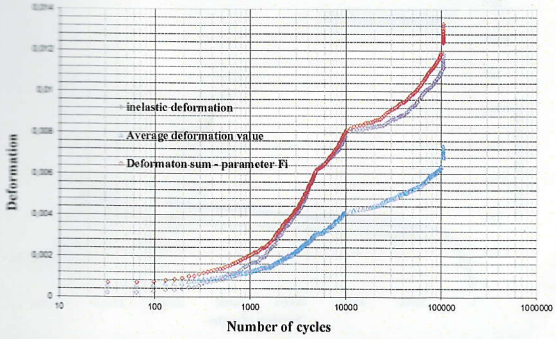

Fig.7 Changes in the development of strain during the subsequent load cycles in the uncoated IN 740 sample at the stress amplitude of 550MPa.

(Fig.9). The same can be observed in the dynamics of the strain development whose variation with increasing stress amplitude has an almost linear character.

In the case of the aluminized specimens, the changes of the fatigue parameters are similar, but the number of cycles to rapture is higher irrespective of the stress amplitude. Changes of the parameter ϕ observed at stress amplitude of 550MPa are shown in **Fig.10**. The results clearly indicate that the fatigue strength of the specimen with the aluminide coating is increased compared to that of the uncoated specimen since the rupture occurs after a greater number of cycles.

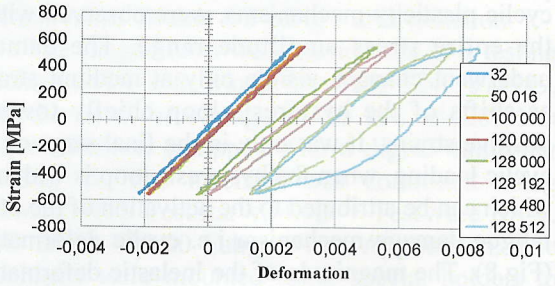

Fig.8 Development of fatigue hysteresis loops during selected cycles in IN 740 coated with an AlNi, intermetallic layer at the stress amplitude of 550 MPa.

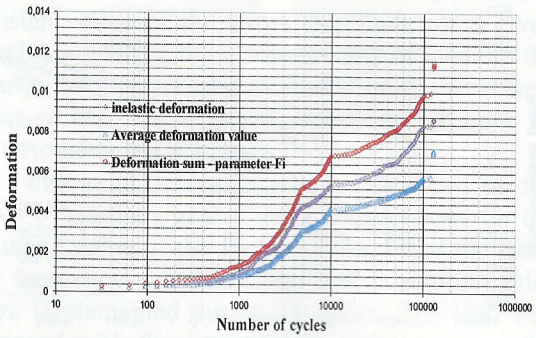

Fig.9 Changes in the development of strain during subsequent load cycles, determined in IN 740 with an AlNi intermetallic layer at the stress amplitude of 550 MPa.

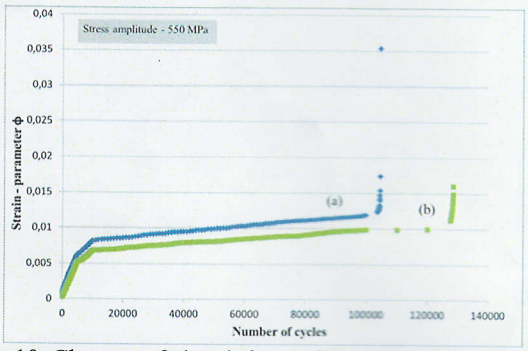

Fig.10 Change of the deformation parameter during the subsequent cycles in the IN 740 nickel alloy: (a) in the initial state, (b) with an AlNi layer, stress amplitude - 550 MPa.

Examinations of the corrosion resistance performed by the potentiodynamic method (**Figs. 11** and **12**) have shown that the corrosion resistance of the aluminized IN 740 nickel alloy is higher than that of the uncoated alloy. It follows from Fig.11 that, within a wide potential range, both materials are in the passive state. The substantial increase of the current density observed in both materials at a potential of about +700mV can be attributed to the evolution of oxygen from water at this potential.

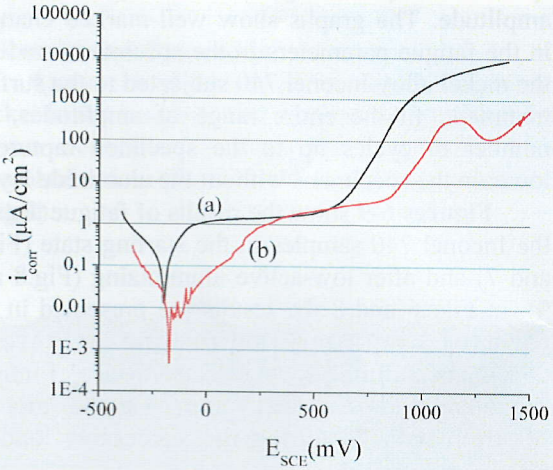

Fig.11 Polarization curves obtained for the uncoated – (a) and aluminized – (b) IN 740 alloy in 0.1M Na_2SO_4 at room temperature.

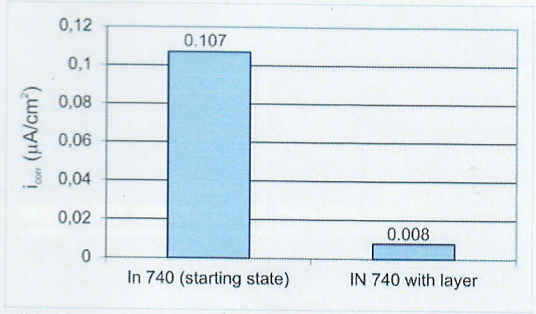

Fig.12 Corrosion current density.

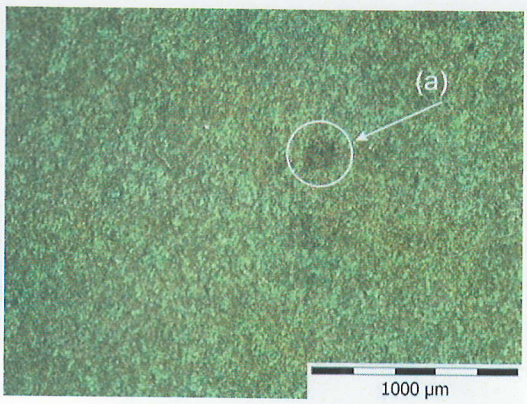

Fig.13 Surface topography of the aluminized IN 740 nickel alloy: (a) area of pitting corrosion after potentiodynamic tests.